Synthetic Peptide Model of an Essential Region of an Aminoacyl-tRNA Synthetase†

Soon Jae Park,‡ W. Todd Miller, and Paul Schimmel*
Department of Biology, Massachusetts Institute of Technology, Cambridge, Massachusetts 02139
Received June 12, 1990

ABSTRACT: A 40 amino acid sequence of the unsolved structure of *Escherichia coli* alanine–tRNA synthetase is essential for tRNA binding and encodes an immunological determinant that cross-reacts with antibodies raised against a eukaryote (insect *Bombyx mori*) alanine enzyme. The secondary structure of this sequence is predicted to be an amphiphilic α-helix that includes one aspartyl and eight glutamyl side chain carboxyl groups. The antibody reactivity and the conformation of a synthetic peptide model of this region (Glu346 to Ser385) were investigated. In addition, double Arg → Gln and Leu → Ala substitutions were separately placed in the enzyme on the hydrophilic and hydrophobic face, respectively, of the predicted helix. These mutations conserve the polar/nonpolar character of each face and retain the potential for helix formation. Circular dichroism spectra of the synthetic peptide model demonstrate the potential for amphiphilic helix formation for the segment from Glu346 to Ser385. The behavior of the mutations in the enzyme, together with earlier data and immunological assays presented here, suggests that one face of the putative helix is an antigenic region of the surface of the enzyme where it contributes to the interaction with alanine tRNA and that the specific sequence of the helix is an important determinant of enzyme stability.

Escherichia coli alanine–tRNA synthetase is an α_4 tetramer of identical subunits of 875 amino acids (Putney et al., 1981a,b). In earlier studies, 18 fragments of *E. coli* alanine–tRNA synthetase were created by gene deletions, and an analysis of these proteins established that the enzyme is organized as a modular arrangement of functional domains (Jasin et al., 1983; Regan et al., 1986). An amino-terminal domain was shown to execute alanyl adenylate synthesis, and sequences added to the C-terminal side of this domain were shown to confer aminoacylation of alanine tRNA. A domain for oligomerization of the tetrameric protein is located in the C-terminal portion of the protein. Evidence was also obtained for a site within the adenylate synthesis domain that interacts with the 3′ end of bound $tRNA^{Ala}$ (Hill & Schimmel, 1989).

The organization of alanine–tRNA synthetase suggested by molecular dissection is thought to be representative of that of most synthetases. Three-dimensional structures have been obtained for *Bacillus stearothermophilus* tyrosine–tRNA synthetase (Brick et al., 1989) and *E. coli* methionine– (Brunie et al., 1987; Zelwer et al., 1982) and glutamine–tRNA synthetases (Rould et al., 1989). While only the amino-terminal half of the 419 amino acid subunit of the dimeric tyrosine enzyme has been solved to atomic resolution, this portion encodes a dinucleotide fold that is the site of tyrosyl adenylate synthesis (Blow et al., 1983). The C-terminal half of the protein is required for recognition of $tRNA^{Tyr}$ (Waye et al., 1983) and contains α-helical segments whose atomic structures and tertiary arrangements have not been clarified.

The methionine and glutamine enzymes also form dinucleotide folds in their respective amino-terminal halves and have structural elements important for tRNA recognition in their C-terminal portions. Although the molecular basis for interaction with tRNA of the predominantly helical C-terminal half of methionine–tRNA synthetase is unknown, the glutamine enzyme was solved as a cocrystal with $tRNA^{Gln}$ (Rould et al., 1989). A domain that is inserted into the nucleotide fold interacts with the acceptor helix and 3′ end of $tRNA^{Gln}$, while a C-terminal β-sheet element encodes determinants that interact with the anticodon in a way that is still to be clarified.

Although a crystal that diffracts to at least 3 Å has been obtained for an amino-terminal fragment of *E. coli* alanine–tRNA synthetase (Frederick et al., 1988), there is no detailed structural information yet available. In an attempt to develop models for this and other proteins of unknown structure, molecular modeling guided by sequence comparisons and secondary structure predictions has been used with some success to establish operational models for limited segments or domains (Starzyk et al., 1987; Clarke et al., 1988; Burbaum et al., 1990). Toward this objective, we have concentrated on a short segment of *E. coli* alanine–tRNA synthetase which is essential for in vitro binding of tRNA and which coincidently encompasses an epitope that uniquely cross-reacts with antibodies raised against a eukaryote alanine enzyme (Regan et al., 1986, 1987).

A monomeric amino-terminal fragment of 461 amino acids has full adenylate synthesis activity and a reduced activity for aminoacylation. When this fragment is expressed from a multicopy plasmid, no other source of alanine–tRNA synthetase is required to sustain the growth of an *alaS* null strain. The reduced k_{cat}/K_m for aminoacylation is at least partly due to a reduced affinity for $tRNA^{Ala}$ (Regan et al., 1986). The affinity is further reduced as additional C-terminal sequences are removed, but the most dramatic effect is caused by the removal of 17 amino acids that encompass Thr369 to Ser385. Removal of these 17 amino acids causes a greater than 100-fold drop in affinity and eliminates detectable tRNA binding in vitro, although the residual 368 amino acid fragment has full adenylate synthesis activity (Regan et al., 1987).

This same region was implicated in an independent study of cross-reacting epitopes on the *E. coli* enzyme. Antibodies raised against silkworm *Bombyx mori* alanine–tRNA synthetase cross-react with the *E. coli* protein. A study of the reactivity of *E. coli* enzyme fragments that had internal and C-terminal deletions of polypeptide sequences showed that only those fragments which encoded Arg350 to Ser385 could

† Supported by Grants GM 15539 and GM 37641 from the National Institutes of Health and by a postdoctoral fellowship from the American Cancer Society to W.T.M.
‡ Present address: Lucky Central Research Institute, Daejeon, Korea.

0006-2960/90/0429-9212$02.50/0

cross-react with the anti *B. mori* enzyme antibodies (Regan et al., 1986). The residues critical for cross-reactivity within this segment were not identified.

Collectively, these previous results suggested that at least part of the tRNA binding site is antigenic and is conserved in evolution. Also conserved in evolution is the use of the same site—a G3·U70 base pair in the acceptor helix—as the major determinant for the identity of *E. coli*, *B. mori*, and human alanine tRNAs (Hou & Schimmel, 1988, 1989). While there is no reason to believe that the segment from Arg350 to Ser385 is involved with recognition of G3·U70, the idea that much of system for recognition is conserved in the alanine case provides motivation for obtaining more detailed information about one particular region of the protein that does play a role in recognition.

For this purpose, we considered a 40 amino acid region from Glu346 to Ser385. This region is predicted to have a propensity for formation of an amphiphilic α helix. To test this prediction and its consequences, we synthesized a 40 amino acid peptide and investigated its helix-forming ability. In addition, point mutations were placed in the full-length protein that preserve the helix-forming and amphiphilic character of this region, but test for sensitivity of the proposed structure to subtle changes on the putative hydrophobic and hydrophilic faces. The experiments demonstrate the capacity for helix formation and cross-reactivity of this small region as an isolated unit and suggest that the stability of the full-length intact protein is sensitive to even small changes in the sequence of this region.

Experimental Procedures

Materials. Trifluoroethanol and *d*-10-camphorsulfonic acid were purchased from Aldrich Chemical Co. Bovine serum albumin, egg albumin, soybean trypsin inhibitor, and cytochrome *c* were obtained from Sigma. The materials necessary for ELISA determinations were purchased from Biolab. The amino acid cartridges and the reagents for peptide synthesis were purchased from Applied Biosystems.

The rabbit polyclonal antibodies raised against *B. mori* alanine aminoacyl-tRNA synthetase were kindly provided by Dr. John Dignam (Medical College of Ohio). The 461- and 699-polypeptide fragments of the *E. coli* Ala-tRNA synthetase were purified according to the methods described by Regan (1986).

Peptides. The 20 amino acid oligopeptide (amino acid sequence Phe366 to Ser385 of *E. coli* Ala–tRNA synthetase) was synthesized by using an Applied Biosystems peptide synthesizer (Model 430A). The software for the peptide synthesis was provided by the manufacturer (version 1.40), and it was used without modification. The average and overall step yields were 99.42% and 89.56%, respectively. The peptide was removed from the resin by treatment with trifluoromethylsulfonic acid (protocol provided by Dr. Sarah McGurdy at Applied Biosystems, Inc., and further modified by Dr. Peter Kim at MIT) and was purified on a C18 reverse-phase HPLC column (Vydac). The crude peptide was loaded onto the column in 0.05% TFA, and a linear gradient to 70% acetonitrile in 0.035% TFA was run. The main peptide peak was collected and lyophilized several times against distilled water.

The 40 amino acid peptide (amino acid sequence from Glu346 to Ser385 of Ala–tRNA synthetase) was synthesized and purified by Dr. David Davis and Dr. Lynn Zieski at Applied Biosystems. The purified peptide was investigated by fast atom bombardment mass spectrometry in Professor K. Biemann's laboratory at MIT and showed the expected ionization pattern. Amino acid sequencing was also used to identify the first five residues of the N-terminal sequence of the 20-mer and of the 40-mer.

The concentration of each purified synthetic peptide was determined by the microbiuret assay (Itzhaki & Gill, 1964) with a modification for small scale. A standard curve was obtained with bovine serum albumin, and distilled water was used for all the reactions to avoid buffer interference. Amino acid analysis was also used to test the peptide concentration obtained by the microbiuret assay (Riordan & Giese, 1977). A known concentration of norleucine was mixed with the peptide solution and hydrolyzed in 6 N HCl at 110 °C. The hydrolysates were analyzed on a Durrum 500 amino acid analyzer. The peptide concentration was calculated by comparing the peak areas of some amino acids with that of norleucine. Because the difference in peptide concentrations by the two methods was within 25%, the average of the two values was taken as the peptide concentration. Once the concentration of the stock peptide solution was determined, aliquots were stored at −20 °C.

Circular Dichroism. CD spectra of the peptides were obtained with an Aviv Model 60DS CD spectrophotometer equipped with a temperature-controlled cell holder (Dr. Peter Kim's laboratory, Whitehead Institute, MIT). Cylindrical quartz cells were used with different light-path lengths (from 0.1 to 10 mm), depending on the concentration of the peptide. The observed CD spectra were corrected on the basis of the calibrated value with camphorsulfonic acid. The blank spectrum was measured and subtracted from the peptide spectrum (Chen & Yang, 1977).

Concentration-dependent helix formation was studied at 25 °C in a buffer of 50 mM potassium phosphate, pH 5.2. For investigation of the pH dependence of the helix–coil transition, the peptide solution in water was mixed with an equal volume of 2.0 mM sodium citrate–boric acid–sodium phosphate/0.2 M sodium chloride (with a preadjusted pH value). The pH of the solution was measured after mixing to correct for minor pH fluctuations.

Molecular Weight Determination. To determine the stoichiometry for association of helices, the molecular weight of the peptide was determined by chromatography on a Sephadex G100 column (1.2 × 98 cm). The column was calibrated with blue dextran, bovine serum alumin, egg albumin, soybean trypsin inhibitor, and cytochrome *c* in 50 mM sodium acetate/0.1 M NaCl (pH 5.0). The protein peaks were monitored at 254 nm (ISCO VA5 detector). The tetradecamer (50 mg/mL) was applied to the column with blue dextran or BSA.

Immunological Assays. Enzyme-linked immunoassay (ELISA) was used to determine the antibody recognition of synthetic peptides by anti *B. mori* Ala–tRNA synthetase antibodies. A 50-μL aliquot of a 10 μg/mL solution of the monomeric amino-terminal fragment of 699 amino acids (699N) in 50 mM sodium bicarbonate (pH 9.6) was applied to the wells of a microtiter plate and left overnight at 4 °C. For the coating with peptides, the peptide solution (40 μg/mL) was dried overnight, fixed with methanol, and washed with phosphate-buffered saline (pH 7.3). The antibodies were diluted, and the reaction with antigen was allowed to proceed for 1 h. Horseradish peroxidase (HRP)-conjugated goat anti-rabbit IgG was used as the secondary antibody with a 1000-fold dilution of the stock solution provided by the manufacturer (Biolab). The microtiter plate was placed on a plate auto-reader (Dynatech Model 550), and the absorbance at 490 nm was measured. All other procedures were followed as recommended by the manufacturer.

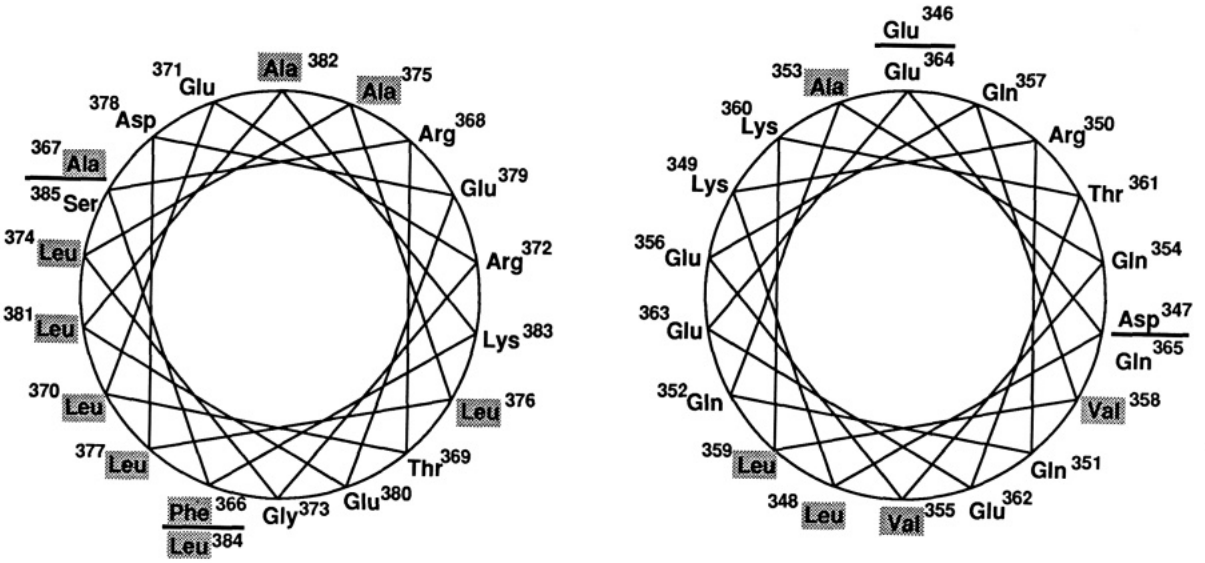

FIGURE 1: Helical wheel projections of the sequences Glu346–Gln365 (right) and Phe366–Ser385 (left). The numbering next to the amino acids is taken from the sequence of *E. coli* Ala–tRNA synthetase. The N-terminal amino acid, Glu346, is located on the top of the right-hand helical wheel. The C-terminal helical wheel is oriented as if a continuous α-helix were formed from Glu346 to Ser385. Hydrophobic side chains are shaded in the figure.

Aminoacylation of Alanine tRNA by Ala–tRNA Synthetase. The biological activity of the synthetic peptides was investigated by testing for inhibition of the aminoacylation reaction. The assay conditions were adapted from the procedure described in Schreier and Schimmel (1972) with several modifications. The assay was done in 25 mM sodium acetate, 80 mM KCl, 10 mM MgC_2, 2 mM DTT, 2 mM ATP, and 20 μM [^{3}H]alanine at pH 5.5 or in 100 mM Tris buffer at pH 8.0. At a fixed concentration of fragment 461N (amino-terminal 461 amino acid polypeptide), increasing amounts of the synthetic peptides were added to the assay buffer. Aliquots were withdrawn and spotted on Whatman filter pads. The reactions were stopped immediately by transferring pads to cold 5% (v/v) trichloroacetic acid. The pads were washed successively by transferring to cold ethanol 3 times and then dried under a heat lamp. The radioactively labeled $tRNA^{Ala}$'s were measured in a Beckman liquid scintillation counter.

Construction of Mutant Ala–tRNA Synthetases. The double substitutions R368Q/R372Q and L370A/L377A were introduced into Ala–tRNA synthetase by using the Amersham oligonucleotide-directed in vitro mutagenesis system. The *alaS* gene was cloned into the *Eco*RI site of the single-stranded DNA phage M13mp18. The mutagenic oligonucleotide primers 5′-ACGCCAGACCCTGCTCCAGAGTCTGAGCAAACTG (R368Q/R372Q) and 5′-GCTCTTCATCCGCCAACGCCAGACCGCGCTCCGCAGTACGAGCA (L370A/L377A) were synthesized on an Applied Biosystems Model 380B DNA synthesizer. The underlined bases indicate the mismatches with the *alaS* coding sequence. After being screened by DNA sequencing with the dideoxynucleotide termination method, the mutants were subcloned from M13 vectors into the *Eco*RI site of pUC19. The resulting plasmids are pTM82 and pTM07 which encode the R368Q/R372Q and L370A/L377A mutants, respectively. Plasmid pTM111 was constructed by cloning the wild-type Ala–tRNA synthetase into the *Eco*RI site of pUC19.

Results

Predicted Helical Structure of Peptide. The amino acid sequence of *E. coli* Ala–tRNA synthetase was analyzed for potential secondary structural domains by using the Chou and Fasman (1978) method. The entire sequence from Ser343 to Asp387 was predicted to have a strong propensity for α-helix formation. Particular emphasis was placed on the region from Arg350 to Ser385 which encompasses the aforementioned cross-reacting epitope and on the segment Thr369 to Ser385 that is important for tRNA binding (Regan et al., 1986, 1987).

Figure 1 shows the amino acid sequence from 346 to 385 viewed on a two-dimensional projection. Portions of this peptide display a segregation of hydrophobic and hydrophilic residues to opposite faces of the helix. There are eight glutamyl and one aspartyl side chain carboxyl groups. When viewed on a helical net diagram (not shown), each one is aligned with one of the six basic side chains (arginine or lysine) where in principle a salt bridge might be formed. The arrangement of amino acids also includes a band of leucine residues on one face of the helix surface which extends for four turns.

In order to assess whether this amphiphilic α-helix plays a functional role in Ala–tRNA synthetase, synthetic peptide models of this region were made by using solid-phase methodology. One peptide is a 20-mer that extends from Phe366 to Ser385 and thus encompasses the C-terminal half of the structure shown in Figure 1, and which is implicated as a determinant for tRNA binding. The other peptide is a 40-mer that encompasses the entire sequence from Glu346 to Ser385.

Immunological Assays. Previous immunological assays showed that the *alaS* protein fragments which contained the region between Arg350 and Ser385 uniquely cross-reacted with rabbit antibodies raised against *B. mori* Ala–tRNA synthetase (Regan et al., 1986). Fragments which encoded deletions of Arg350 to Ser385 did not cross-react. The ELISA experiments with peptide antigens were done with the same antibodies as were used for the previous study.

The antibodies recognize the synthetic 20 amino acid peptide as well as the 40-mer (Figure 2). The sensitivity is about 1000-fold greater with the monomeric *alaS* protein fragment 699N than with the peptides (which appear to be equivalent). This suggests that the main cross-reacting epitope is in the 20-mer segment from Phe366 to Ser385.

The diminished reactivity of a peptide antigen as compared to its counterpart in the protein is common (Jemmerson &

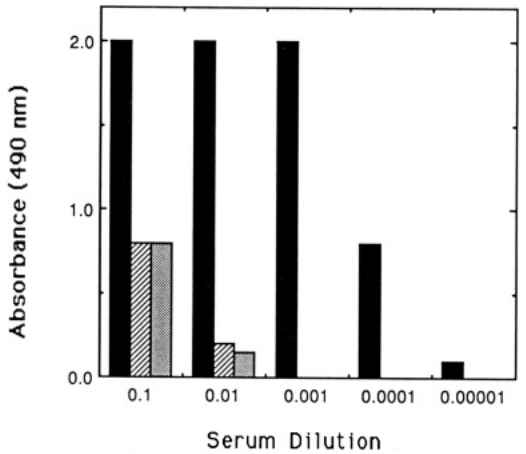

FIGURE 2: Immunological response of the synthetic peptides and of a large polypeptide fragment of *E. coli* Ala-tRNA synthetase. The experimental conditions for this ELISA assay with anti *B. mori* alanine-tRNA synthetase antibodies (Regan et al., 1986) were as described under Experimental Procedures. The solid bar represents the result obtained with fragment 699N. The hatched bar and the dotted bar indicate the antibody reactions with the 40-mer and the 20-mer, respectively. The background absorbance was obtained from the experiment with preimmune serum and was subtracted from the one obtained with immune serum.

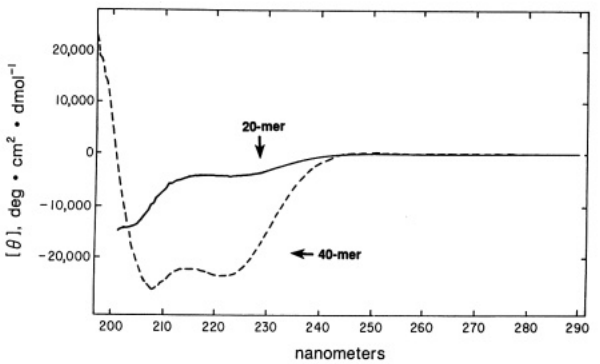

FIGURE 3: CD spectra of the synthetic peptides. The mean ellipticity, $[\theta]$, is plotted versus wavelength. Spectra were measured in 50 mM potassium phosphate, pH 5.2. The concentration of the 20-mer was 500 μg/mL; similar CD spectra were obtained at different peptide concentrations in the range 50–500 μg/mL. The concentration of the 40-mer was 800 μg/mL. The two minima in $[\theta]$ at 209 and 222 nm were evident for the 40-mer at concentrations below 80 μg/mL (cf. Figure 5). The CD spectra shown here are the averages of three scans at 23 °C.

Paterson, 1986). Among other possibilities, the reduced sensitivity for recognition of the synthetic peptides could be a result of reduced efficiency of coating of the microtiter plate as compared to the protein 699N.

Helix Formation in Tetradecamer. The circular dichroism spectrum of the Phe366 to Ser385 20-mer showed no significant secondary structure, either over a broad range of pH conditions or over the concentration range of 50–500 μg/mL (Figure 3). In contrast, the Glu346 to Ser385 synthetic 40-mer has a circular dichroism spectrum at pH 5.2 that is typical of that for an α-helix. On the basis of the Chen and Yang (1977) formulation, approximately 75% of the peptide is in a helical conformation under these conditions.

The formation of helical structure is strongly pH dependent, with random coil like structure forming above the transition midpoint of pH 6.8 (Figure 4). The pH profile operationally behaves like the titration of a single group and may indicate a critical role in helix stability for Asp347 or one of the eight glutamic acid residues. The pH-dependent formation of α-helix structure in glutamic acid containing homo- and co-

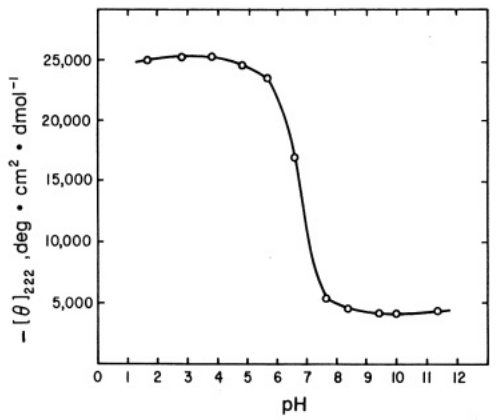

FIGURE 4: Helix formation of the 40 amino acid peptides as a function of pH. The peptide solution (0.8 mg/mL) was made with 1 mM sodium citrate–boric acid–sodium phosphate/0.1 M sodium chloride. The path length of the cell was 0.1 mm, and the spectra were measured at 222 nm.

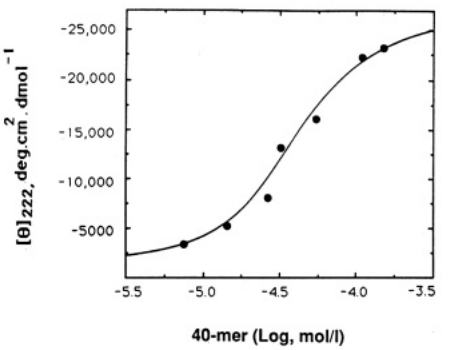

FIGURE 5: Helix formation of the 40-mer at various concentrations. Peptide solutions were made in 50 mM potassium phosphate at pH 5.2, 23 °C. The path length of the cell was 0.1 or 1.0 mm depending on the ionic strength of the solution.

polymers has been well established (Holzwarth & Doty, 1965; Adler et al., 1968). The elevated apparent pK value corresponds to a stabilization (by the helix) of the protonated form by 2.0–2.5 kcal/mol.

Helix formation is also concentration dependent. A systematic study over the range of 35–700 μg/mL indicates that an intermolecular interaction between peptides promotes helix formation (Figure 5). A computer simulation of the concentration dependence of helix formation gave an empirical Hill coefficient of $n = 2$ [cf. pp 863–866 of Cantor and Schimmel (1980)]. This empirical analysis suggests that association of at least two peptides is needed to stabilize the helix.

To confirm the formation of a helical bundle, the apparent molecular weight of the 40-mer was measured by chromatography on a Sephadex G100 column at pH 5.0. The helical peptide chromatographs as a single peak with an apparent molecular weight of 26 000 (Figure 6). The random coil like peptide at pH 7.5 has an apparent molecular weight of 4660. The number of helical peptides that are associated at pH 5.0 cannot be counted with accuracy because of the uncertainty in the hydrodynamic radius of a helical bundle which could be large due to the asymmetry of the associated complex. Nonetheless, the chromatography results are consistent with an association of helical units. Preliminary results of ultracentrifugation experiments with Dr. W. Stafford (Boston Biomedical Research Institute) confirmed the association between helical peptide species.

The results suggest that the strong tendency for helix formation of the 40-mer is dependent on association between

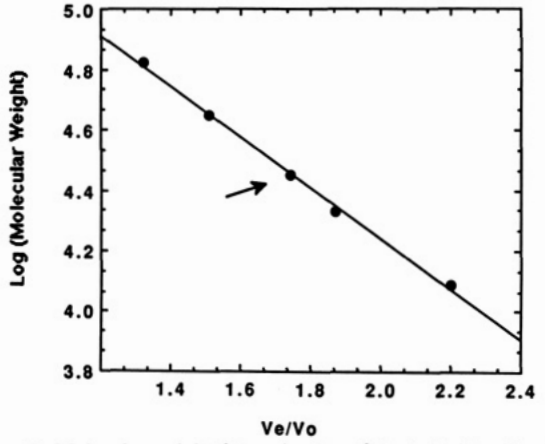

FIGURE 6: Molecular weight determination of the helical bundle. The Sephadex G100 column (1.2 × 97 cm) was equilibrated with 50 mM sodium acetate/0.1 M sodium chloride at pH 5.0 and calibrated with bovine serum albumin (66 000), ovalbumin (42 700), soybean trypsin inhibitor (21 500), and cytochrome *c* (12 400). Blue dextran and ATP were used to estimate the void volume (V_e) and total volume (V_t) of the column, respectively. The peptide concentration was 25 mg/mL, and 400 μL of this solution was loaded onto the column.

helices, perhaps as a result of contacts between the hydrophobic clusters (e.g., the four leucines in the C-terminal half) that are on one face. The lack of helix formation observed for the 20-mer is consistent with the strong dependency of cooperative helix formation on chain length, especially for peptides that are under 50 amino acids in size [see pp 1041–1073 of Cantor and Schimmel (1980)].

Amino Acid Substitutions in Putative Helix of Ala–tRNA Synthetase. To test the hypothesis that the amphiphilic helix spanning Phe366 to Ser385 of Ala–tRNA synthetase plays an important functional and/or structural role, we constructed the double mutants R368Q/R372Q and L370A/L377A via oligonucleotide-directed mutagenesis as described under Experimental Procedures. These conservative amino acid replacements are predicted to preserve the helicity and amphiphilicity in this region and do not introduce steric conflicts in the structure. The phenotypes of these mutations were tested in the *E. coli alaS* deletion strain W3110 (Jasin & Schimmel, 1984). This strain is maintained by plasmid pMJ901, which encodes wild-type *alaS* and has a temperature-sensitive replicon which causes plasmid loss at 42 °C.

The *alaS* mutants were introduced into W3110 on the compatible plasmids pTM82 and pTM07, and the transformants were tested for complementation at 42 °C. Neither mutant complemented the growth-defective phenotype of W3110 at 42 °C, while wild-type *alaS* does complement W3110 (Figure 7, top). This indicates that, while the substitutions in pTM82 and pTM07 are conservative, they are lethal.

Western blot analysis was carried out on extracts of W3110/pMJ901 cells containing the plasmid-encoded mutants. These extracts were prepared from 200 mL of late log-phase cells that were grown at 30 °C using procedures described previously (Hill & Schimmel, 1989). Aliquots of the extracts were electrophoresed on an SDS–polyacrylamide gel (7.5%), transferred to a poly(vinylidene difluoride) membrane, and immunostained with anti *E. coli* Ala–tRNA synthetase antibodies using the ProtoBlot alkaline phosphatase system (Promega). These experiments indicated that the mutant proteins were unstable and gave little if any protein of the native molecular weight (Figure 7, bottom). A fragment of lower molecular weight (about 66K) accumulated in each case (data not shown), suggesting that the mutants were

FIGURE 7: Behavior of the mutants in the *alaS* deletion strain W3110/pMJ901. (Top) Complementation at 42 °C. Plasmids encoding wild-type (pTM111), R368Q/R372Q (pTM82), or L370A/L377A (pTM07) Ala–tRNA synthetases were introduced into W3110/pMJ901, and transformants were tested for complementation at 42 °C. (Bottom) Western blot analysis of the mutant synthetases. Extracts of W3110/pMJ901 cells containing the appropriate constructs were made as described previously (Hill & Schimmel, 1989). SDS–polyacrylamide gel electrophoresis was carried out, and the bands were electroblotted onto a poly(vinylidene difluoride) membrane and immunostained with anti *E. coli* Ala–tRNA synthetase antibodies. Lane 1, purified Ala–tRNA synthetase; lane 2, W3110/pMJ901/pTM111; lane 3, W3110/pMJ901/pTM82; lane 4, W3110/pMJ901/pTM07; lane 5, W3110/pMJ901.

partially degraded. In contrast, plasmid-encoded wild-type *alaS* directed synthesis of a stable protein (of the expected size) that is easily detected by immunostaining (Figure 7, bottom).

Discussion

The experiments reported here test a specific structural prediction for a region of functional importance in *E. coli* Ala–tRNA synthetase. Earlier modeling and mutagenesis of the Met– and Ile–tRNA synthetases helped to define sequences which play particular structural roles in these proteins. For example, a dinucleotide fold that is split by insertion of a long polypeptide was predicted for *E. coli* Ile–tRNA synthetase (Starzyk et al., 1987). This prediction was supported by analysis of the stabilities and activities of members of a set of internal deletion mutants. Regions of Met–tRNA synthetase important for the dinucleotide fold structure and its associated activity have also been mapped via insertion mutagenesis (Starzyk et al., 1989).

Chou–Fasman analysis of the amino acid sequence of *E. coli* Ala–tRNA synthetase suggested several long regions of α-helical structure. The most prominent regions encompass residues 102–148, 343–385, and 458–502. Because most of the segment from Lys458 to Ser502 is outside of the region that is essential for catalytic activity (Regan et al., 1987), it is of less interest than the other two which are within the catalytic core of the enzyme. The potential α-helix that spans amino acids Ser343 to Ser385 was of particular interest (see above), and a two-dimensional projection showed that it had significant amphiphilic character (Figure 1). The specific alignment of positively and negatively charged side chains would also be expected to stabilize an α-helix, as has been observed in model peptides (Marqusee & Baldwin, 1987).

While no significant secondary structure was detected in the Phe366–Ser385 20-mer, the Glu346–Ser385 40-mer has a concentration-dependent helical structure (Figure 5). These results and hydrodynamic data indicate that the 40 amino acid peptide has a strong tendency to form intermolecular aggregates. This may be due in part to the pattern of leucine residues present on the hydrophobic faces of the helices (Figure 1). It is unknown whether this region of the protein plays a role in formation of the tetrameric quaternary structure of the enzyme. However, amino-terminal fragments that extend to Gly699 are monomeric (Jasin et al., 1983), so that the region from Glu346 to Ser385 is not sufficient for formation of a stable tetramer. In particular, a determinant that maps between Gly699 and Glu808 is required for tetramer formation (Jasin et al., 1983), although other parts of the polypeptide, such as Glu346–Ser385, may cooperate to stabilize the quaternary structure.

Deletion analysis of Ala-tRNA synthetase has also shown that the segment from Thr369 to Ser385 directly or indirectly contributes at least 25% of the free energy of association between enzyme and tRNA (Regan et al., 1987). This region is closely associated with the domain for adenylate synthesis which extends from the amino terminus to Arg368. The interaction of a small region in the adenylate synthesis domain of a synthetase with its cognate tRNA is observed in the cocrystal of *E. coli* Gln-tRNA synthetase with $tRNA^{Gln}$ (Rould et al., 1989). In this system, the carboxyl side chain of Asp235 hydrogen bonds to the exocyclic 2-amino group of G3 in the minor groove of the acceptor helix of $tRNA^{Gln}$. Possibly one or more of the exposed side chains on the hydrophilic face of the putative α-helix of Ala-tRNA synthetase makes contacts with $tRNA^{Ala}$.

The in vitro binding of the synthetic peptides to $tRNA^{Ala}$ was tested by inhibition of the aminoacylation reaction of fragment 461N (data not shown). The binding constant of 461N to $tRNA^{Ala}$ is approximately 20 times weaker than that of the native enzyme (Regan et al., 1987). Significant inhibition of aminoacylation (about 40%) was observed at concentrations of the 40-mer of 360 μM at pH 5.5. At this peptide concentration, the solution became turbid as a result of coprecipitation of tRNA and the 40-mer. The precipitates only formed when peptide and tRNA were mixed, suggesting that a strong interaction occurred between the two species. At pH 7.5, where helix formation is suppressed, no precipitation occurred, and much less inhibition of aminoacylation was observed. Because it is possible that the inhibition of aminoacylation at lower peptide concentrations was due to incipient precipitation not visible to the eye, we were reluctant to pursue further this aspect of the analysis.

Having established that the Glu346–Ser385 peptide can adopt an α-helical structure, we introduced amino acid changes (R368Q/R372Q and L370A/L377A) on both faces of the putative helix by site-directed mutagenesis of the full-length protein. Plasmids that encode these mutant synthetases were unable to function in vivo, as judged by their inability to sustain growth at 42 °C of an *alaS* null strain. By comparison, plasmids that encode fragment 461N of the Ala-tRNA synthetase, which has a k_{cat}/K_m for aminoacylation reduced about 1000-fold relative to the wild-type enzyme, are able to complement the *alaS* null strain, as are plasmids that encode the activity-deficient *alaS4* and *alaS5* point mutants (Ho et al., 1985; Jasin et al., 1983).

The contribution of amphiphilicity to biological function has been well characterized in peptide systems (Kaiser & Kezdy, 1984). In many cases, it has been possible to synthesize functional peptide analogues which have little homology to the naturally occurring peptide but which preserve the distribution of hydrophobic and hydrophilic residues. It was observed in these studies that peptides containing hydrophobic faces composed entirely of leucine residues often form stronger amphiphilic secondary structures than the natural peptides on which they were based. Accordingly, it was expected that the double mutation L370A/L377A in Ala-tRNA synthetase would perturb the hydrophobic face in this region. As for the R368Q/R372Q mutation, it was our expectation that the removal of two positive charges on the hydrophilic face of the helix might disrupt a potential interaction with the tRNA substrate. Both mutations in the synthetase abolished biological activity, suggesting that relatively minor perturbations in this structural motif can render it nonfunctional. However, the failure of the R368Q/R372Q and L370A/L377A mutants to complement may be due to a loss of activity that accompanies protein degradation or, additionally or alternatively, to a deficient activity in the full-length protein prior to its degradation in vivo.

The hypothesis that the amphiphilic helix plays a role in tRNA recognition could be tested by in vitro tRNA filter binding studies with the mutant proteins. Mutations in the helix such as R368Q/R372Q and L370A/L377A would be expected to reduce the affinity of this interaction. This analysis, however, would depend on the purification of the truncated forms of the mutant proteins, and it is not clear whether the degraded products retain the region of interest.

Acknowledgments

We thank Dr. Lynn Zieski (Applied Biosystems, Inc.) and Dr. David Davis (presently at Athena Neurosciences, Inc.) for synthesis, purification, and characterization of the 40 amino acid peptide.

References

Adler, A. J., Hoving, R., Potter, J., Wells, M., & Fasman, G. D. (1968) *J. Am. Chem. Soc. 90*, 4736.

Blow, D. W., Bhat, T. N., Metclafe, A., Risler, J. L., Brunie, S., & Zelwer, C. (1983) *J. Mol. Biol. 171*, 571–576.

Brick, P., Bhat, T. N., & Blow, D. W. (1989) *J. Mol. Biol. 208*, 83–98.

Brunie, S., Mellot, P., Zelwer, C., Risler, J.-L., Blanquet, S., & Fayat, C. (1987) *J. Mol. Graphics 5*, 18–21.

Cantor, C. R., & Schimmel, P. R. (1980) *Biophysical Chemistry*, W. H. Freeman & Co., San Francisco.

Chen, G. C., & Yang, J. T. (1977) *Anal. Lett. 10*, 1195–1207.

Chou, P. Y., & Fasman, G. D. (1978) *Adv. Enzymol. 47*, 45–148.

Frederick, C. A., Wang, A. H.-J., Rich, A., Regan, L., & Schimmel, P. (1988) *J. Mol. Biol. 203*, 521–522.

Hill, K., & Schimmel, P. (1989) *Biochemistry 28*, 2577–2586.

Holzwarth, G. M., & Doty, P. (1965) *J. Am. Chem. Soc. 87*, 218.

Itzhaki, R. F., & Gill, D. H. (1964) *Anal. Biochem. 9*, 401–410.

Jasin, M., & Schimmel, P. (1984) *J. Bacteriol. 159*, 783–786.

Jasin, M., Regan, L., & Schimmel, P. (1983) *Nature 306*, 441–447.

Jemmerson, R., & Paterson, Y. (1986) *BioTechniques 4*, 18–31.

Kaiser, E. T. & Kezdy, F. J. (1984) *Science 223*, 249–255.

Marqusee, S., & Baldwin, R. L. (1987) *Proc. Natl. Acad. Sci. U.S.A. 84*, 8898–8902.

Park, S. J., Hou, Y.-M., & Schimmel, P. (1989) *Biochemistry 28*, 2740–2746.

Putney, S. D., Royal, N. J., de Vegvar, H. N., Herlihy, W. C., Biemann, K., & Schimmel, P. (1981a) *Science 213*, 1497-1501.

Putney, S. D., Sauer, R. T., & Schimmel, P. (1981b) *J. Biol. Chem. 256*, 198-204.

Regan, L. (1986) Ph.D. Thesis, Massachusetts Institute of Technology.

Regan, L., Dignam, J. D., & Schimmel, P. (1986) *J. Biol. Chem. 261*, 5241-5244.

Regan, L., Bowie, J., & Schimmel, P. (1987) *Science 235*, 1651-1653.

Riordan, J. F., & Giese, R. W. (1977) *Methods Enzymol. 47*, 31-40.

Rould, M. A., Perona, J. J., Söll, D., & Steitz, T. A. (1989) *Science 246*, 1135-1142.

Schreier, A. A., & Schimmel, P. (1972) *Biochemistry 11*, 1582-1589.

Starzyk, R. M., Webster, T. A., & Schimmel, P. (1987) *Science 237*, 1614-1618.

Starzyk, R. M., Burbaum, J. J., & Schimmel, P. (1989) *Biochemistry 28*, 8479-8484.

Waye, M. W., Winter, G., Wilkinson, A. J., & Fersht, A. R. (1983) *EMBO J. 2*, 1827-1829.

Zelwer, C., Risler, L., & Brunie, S. (1982) *J. Mol. Biol. 155*, 63-81.

Cadmium-113 NMR Studies of the DNA Binding Domain of the Mammalian Glucocorticoid Receptor†

Tao Pan, Leonard P. Freedman,‡ and Joseph E. Coleman*

Department of Molecular Biophysics and Biochemistry, Yale University, New Haven, Connecticut 06510, and Department of Biochemistry and Biophysics, University of California, San Francisco, California 94143

Received March 30, 1990; Revised Manuscript Received June 26, 1990

ABSTRACT: The DNA binding domain of the mammalian glucocorticoid hormone receptor (GR) contains nine highly conserved cysteine residues, a conservation shared by the superfamily of steroid and thyroid hormone receptors. A fragment [150 amino acids (AA) in length] consisting of GR residues 407-556, containing within it the entire DNA binding domain (residues 440-525), has been overexpressed and purified from *Escherichia coli* previously. This fragment has been shown to contain 2.3 ± 0.2 mol of Zn(II) per mole of protein [Freedman, L. P., Luisi, B. F., Korszun, Z. R., Basavappa, R., Sigler, P. B., & Yamamoto, K. R. (1988) *Nature 334*, 543]. Zn(II) [or Cd(II) substitution] has been shown to be essential for specific DNA binding. ^{113}Cd NMR of a cloned construct containing the minimal DNA binding domain of 86 AA residues [denoted GR(440-525)] with ^{113}Cd(II) substituted for Zn(II) identifies 2 Cd(II) binding sites by the presence of 2 ^{113}Cd NMR signals each of which integrates to 1 ^{113}Cd nucleus. The chemical shifts of these two sites, 704 and 710 ppm, suggest that each ^{113}Cd(II) is coordinated to four isolated $-S^-$ ligands. Shared $-S^-$ ligands connecting the two ^{113}Cd(II) ions do not appear to be present, since their T_1s differ by 10-fold, 0.2 and 2.0 s, respectively. Addition of a third ^{113}Cd(II) or Zn(II) to $^{113}Cd_2$GR(440-525) results in occupancy of a third site, which introduces exchange modulation of the two original ^{113}Cd NMR signals causing them to disappear. Addition of EDTA to the protein restores the original two signals. ^{1}H-^{113}Cd heteronuclear multiple quantum spectroscopy of GR(440-525) shows that the major protons coupled to ^{113}Cd are a group of β-protons assignable to Cys residues. A small variable signal corresponding to a ϵ-CH_3 of Met coupled to ^{113}Cd suggests that the thioether of a Met may be a ligand to the third ^{113}Cd(II) ion. Binding of the third ^{113}Cd(II) causes significant increase of the Cd-S charge transfer absorption bands. We propose that GR(440-525) can form three Zn(II) binding sites involving a combination of the nine Cys and one Met residues as ligands, all of which are highly conserved among the superfamily of steroid and thyroid hormone receptors. Both circular dichroism and ^{1}H NMR show the folding of GR(440-525) to be dependent on the presence of Zn(II) or Cd(II). Removal of the metal ions causes GR(440-525) to completely unfold from its native structure. Both Zn(II) and Cd(II)GR(440-525) have very similar ^{1}H NMR spectra, suggesting almost identical structures for the two metal derivatives of the DNA binding domain of GR.

The mammalian glucocorticoid hormone receptor (GR)[1,2] belongs to the superfamily of steroid and thyroid hormone receptors which have striking amino acid sequence homologies within their DNA binding domains [for a review, see Evans

† This work was supported by NIH Grants DK09070 and GM21919 and by NSF Grant DMB 8716787 (to Keith Yamamoto). The 500-MHz NMR was supported by NIH Grant RR03475, NSF Grant DMB-8610557, and ACS Grant RD259. This work is in partial fulfillment of the Ph.D. requirements for T.P.

* Address correspondence to this author at the Department of Molecular Biophysics and Biochemistry, Yale University.

‡ Present address: Cell Biology and Genetics Program, Memorial Sloan Kettering Cancer Center, New York, NY 10021. L.P.F. was the recipient of a Bank of America-Giannini Foundation fellowship.

[1] Abbreviations: GR, glucocorticoid hormone receptor; GR(407-556), cloned polypeptide fragment of the mammalian glucocorticoid receptor containing amino acid residues 407-556 which span the DNA binding domain, plus 10 residues on the N-terminus and 14 residues on the C-terminus from the cloning vector; GR(440-525), cloned fragment of GR which contains residues 440-525 plus six residues (MKPARP) on the N-terminus and two residues (RL) on the C-terminus contributed by codons from the cloning vector; TSP, sodium (trimethylsilyl)tetradeuteriopropionate.

0006-2960/90/0429-9218$02.50/0